Holographic fabrication of photonic crystals using multidimensional phase masks

Yuankun Lin,[1,a)] Ahmad Harb,[2] Daniel Rodriguez,[2] Karen Lozano,[2] Di Xu,[3] and K. P. Chen[3]
[1]*Department of Physics and Geology, University of Texas-Pan American, Edinburg, Texas 78539, USA*
[2]*Department of Mechanical Engineering, University of Texas-Pan American, Edinburg, Texas 78539, USA*
[3]*Department of Electrical and Computer Engineering, University of Pittsburgh, Pittsburgh, Pennsylvania 15261, USA*

(Received 17 July 2008; accepted 2 November 2008; published online 4 December 2008)

This paper reports the experimental approaches to the fabrication of two-layer integrated phase masks and the fabrication of photonic crystal templates using the phase mask based on holographic lithography technique. The photonic crystal template is formed by exposing photoresist mixtures to five-beam interference patterns generated through the phase mask. The fabricated phase mask consists of two layers of orthogonally oriented gratings produced in a liquid crystal and photoresist mixture. A polymerization-induced phase separation preserves the grating structure during the exposure. The vertical spatial separation between two layers of gratings produces a phase difference among diffracted laser beams, which enables the holographic fabrication of diamondlike photonic crystal structures. The fabricated photonic crystal structure is consistent with simulations based on the five-beam interference. The two-layer phase mask opens up an opportunity of direct printing photonic structures. © *2008 American Institute of Physics*. [DOI: 10.1063/1.3037234]

I. INTRODUCTION

Photonic crystals are microstructured materials in which the dielectric constant is periodically modulated on a length scale comparable to the desired wavelength of operation.[1,2] It is now possible to produce two-dimensional (2D) photonic crystals[3] at high volume and low cost through the use of deep ultraviolet photolithography, which is the standard tool of the electronics industry. However, a large-scale efficient microfabrication of three-dimensional (3D) photonic bandgap microstructures has been a scientific challenge over the past decade. So far, a number of fabrication techniques such as conventional multilayer stacking of woodpile structures using semiconductor fabrication processes,[4] colloidal self-assembly,[5] and multiphoton direct laser writing[6] have been employed to produce submicron 3D photonic crystals or templates. Holographic lithography based on multibeam interference has recently been employed to fabricate 3D photonic crystals by exposing a photoresist or polymerizable resin to interference patterns of laser beams.[7–20] This multibeam interference technique has produced submicron-scale structures over large substrate areas.[8,9] A diamondlike structure is desirable due to a larger photonic bandgap when compared to a simple face-centered-cubic (fcc) structure and its bandgap robustness to deviations of the structural parameters from their optimum values.[4,10,21] Holographic lithography based on four noncoplanar beams can generate a diamondlike structure with beams from all spaces (360°).[10] Five-beam interference can generate a diamondlike structure with all beams from the same half space by controlling the polarization[15] and phase relation of the interfering beams.[16,17]

Traditionally, multibeam interference holography was realized by a large number of bulk optical components such as mirrors, beam splitters, and lenses.[8,9] In order to improve the stability of optical setup and reduce its complexity, a number of groups have demonstrated the construction of three- or four-beam interferences using a single diffractive[11–13] or deflective[14] optical element. If designed carefully, these single diffractive or deflective optical elements can replace the complex optical setup for the fabrication of photonic crystals based on the holographic lithography.[11–14] For the holographic lithography based on the five-beam interference, a single flat-top prism was demonstrated for the fabrication of diamondlike or woodpile photonic crystals template using a polarization effect with a configuration consisting of four linearly polarized side beams arranged symmetrically around a circularly polarized central beam.[15] Despite its simplicity, the use of a bulk optical element is still not compatible with a standard photolithography-based process currently used in the fabrication of optoelectronic integrated circuits (ICs).

An alternative single-optical-element approach has been demonstrated to produce multiple-beam interference patterns for 3D photonic crystal fabrication. The bulk deflective optical element was replaced by a diffractive optical element such as one-dimensional (1D) or 2D surface gratings or phase masks.[11–13,18–20] Using a 2D phase mask, a single beam can be diffracted into one zeroth order diffraction beam (0,0) and four first order [(0,1), (0,−1), (1,0), and (−1,0)] or higher order beams for 3D holographic fabrication of the photonic crystal.[18]

Since 1D or 2D surface gratings (phase masks) can be conveniently fabricated together with amplitude masks on the same glass plate, it opens up opportunities of direct printing 3D photonic structures together with other optoelectronic elements on chip. Lin *et al.*[18] theoretically proposed a 2D

[a)]Electronic mail: linyk@utpa.edu.

phase mask for generating five-beam interference. The overlapped beams have the same initial phases and therefore will produce an interference pattern with a simple fcc or face-center-tetragonal (fct) symmetry.

However, the formation of diamondlike structures needs to have two first-order counterpropagating beams [for example, (0,1) and $(0,-1)$] shifted in phase by $\pi/2$ relative to others.[17] Thus Chan *et al.*[17] theoretically proposed to "lock" the required phase shift in the mask by fabricating 1D gratings in two layers on the same substrate. The optimized phase shift is determined by the vertical spatial separation between two gratings.[17] The phase mask can be carefully designed to manipulate the phase relations of the diffracted beams and thus their interference pattern can be used to produce photonic crystal templates with diamondlike structures. Another promising method might be electro-optically tunable phase arrays in lithium niobate crystals as a dynamic phase mask which has been tested for coherent diffraction lithography.[19,20]

In this paper, we demonstrate an experimental approach to the fabrication of 2D and multiple-layer phase mask on a single substrate for the generation of five-beam interference pattern. The fabricated multiple-layer optical phase mask consists of two orthogonally oriented gratings and can produce a phase shift among the diffracted beams. The diamondlike photonic crystal template is fabricated by exposing photosensitive polymers through the multiple-layer phase mask lithography.

II. FABRICATION OF MULTIPLE-LAYER PHASE MASK

The photoresist mixtures used for the fabrication of multiple-layer phase mask were similar to a reported formulation (without fatty acid).[22] The following components were used (in weight percentages): dipentaerythritol penta/hexaacrylate (DPHPA) monomer (Aldrich, 65%), BL111 liquid crystal (LC) (EMD Chemicals, 25%), photoinitiator rose bengal (0.3%), coinitiator *n*-phenyl glycine (NPG, 0.5%), and chain extender *n*-vinyl pyrrolidinone (NVP, 9.2%). Figure 1(a) shows an absorption spectrum of the mixture with a peak between 480 and 590 nm from the rose bengal. The addition of the rose bengal makes the photoresist mixture sensitive to selected laser wavelengths. Coherent compass laser (532 nm, 60 mW) was used for the exposure of the photoresist mixture. One laser beam was expanded to a size of 10 mm and separated into two beams using a beam splitter. A parallel fringe is formed when two laser beams overlap. The spacing Λ between the dark (or bright) fringes is determined by the laser wavelength and interference angle β by the relationship of $\Lambda=\lambda/(2\sin\beta)$. When a photoresist is exposed to the interference pattern and developed, it forms a 1D grating on the substrate. In order to fabricate a two-layer grating structure, the LC was mixed with the photoresist. When the photoresist mixture received the laser exposure, a polymerization process occurred in the region under high laser dosage. Due to a well known polymerization-induced phase separation process,[22,23] the LC was pushed toward the region receiving a lower laser dosage as shown in Fig. 1(b). Thus the laser exposed sample consists of a periodic distribution of LC-rich domains, corresponding to the dark regions of the interference pattern, and the polymer-rich grating structure. The LC-rich region has little material for further polymerization. In one of our samples, we mixed LCs inhomogeneously with the photoresist solution. The sample was exposed to the two-beam interference pattern then rotated 90° and exposed to the interference pattern again. After the double exposures, the 1D grating formed under the first laser exposure was protected in the region with high LC concentration while other regions had 2D orthogonal structures, as shown in Fig. 1(c). Thus the addition of LC in the photosensitive mixture helps preserve the grating structure produced in the first exposure.

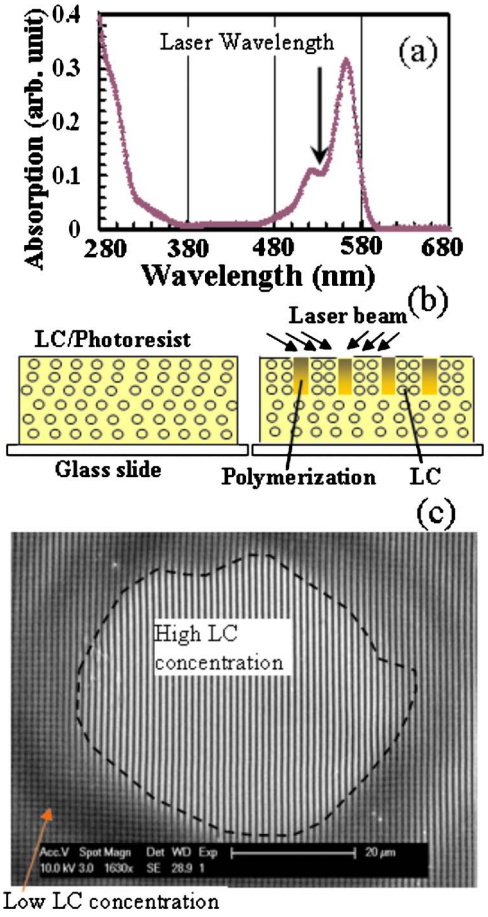

FIG. 1. (Color online) (a) Absorption spectrum of the photoresist mixture. (b) Schematic of laser exposure induced phase separation in a mixture of LC and photoresist. (c) SEM of fabricated structure in a mixture where the LC was inhomogeneously mixed with photoresist.

The above inherent phase separation characteristic played a key role in the fabrication of the two-layer integrated phase mask. For the phase mask fabrication, the mixture was stirred for 8 h and spin coated over a transparent glass slide (Corning) with a typical speed of 4000 rpm. The thickness of the sample is determined by the spin-coating speed. For such a spin-coating speed of 4000 rpm, the typical thickness of the sample is 3 μm. Two laser exposures (532 nm) were performed for the fabrication of phase mask. For the first exposure, two interfering laser beams came from the glass slide side and formed the LC-rich and polymer-rich gratings parallel to the *y*-direction. Because the LC-rich re-

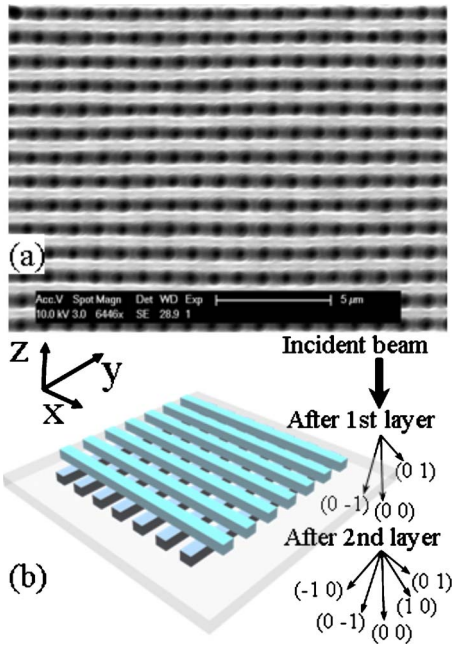

FIG. 2. (Color online) (a) SEM of fabricated multiple-layer phase mask and (b) schematic of laser beam diffraction through the phase mask.

gion is much less sensitive to further laser exposure than the polymer-rich region, more laser exposures will induce weak polymerization in the LC-rich region allowing this region to be washed out during the development. The time for first exposure was in the range of 0.5–2 s. Because the exposure time is short, only the photoresist near the glass slide (substrate) becomes polymerized. Then the same sample was exposed to the laser interference pattern rotated by 90° and coming from the sample side. After an exposure in the range of 2–4 s, a grating parallel to the *x*-direction is formed. The sample was developed in propylene-glycol-methyl-ether-acetate (PGMEA) (Microchem) for 20 s and rinsed in isopropanol.

Figure 2(a) shows the scanning electron microscope (SEM) of the fabricated phase mask showing clearly two layers of grating structures. The top layer has a grating in the horizontal direction. The layer beneath has a grating in vertical direction, orthogonal to the top grating structure. From the scale bar, the period of the grating was measured to be 1.06 μm. The diffraction angle of the 532 nm laser by the grating was measured to be 31°, corresponding to a grating period of 1.03 μm.

III. THEORETICAL DESCRIPTION OF THE PHASE MASK LITHOGRAPHY

When a single beam goes through such a phase mask, it is desirable to have five and only five diffracted beams behind the phase mask, namely, the (0,0), $(0,\pm 1)$, and $(\pm 1,0)$ beams,[17] as shown in Fig. 2(b). The next lowest order beams are the $(\pm 1,\pm 1)$ beams.[17] If the phase mask was designed properly, these four beams vanish. The five low order diffracted beams can be described by

$$\mathbf{E}_{0,0}(\mathbf{r},t) = \mathbf{E}_{0,0}\cos(k_{0,0}\cdot r - \omega t + \delta_1), \quad (1)$$

$$\mathbf{E}_{1,0}(\mathbf{r},t) = \mathbf{E}_{1,0}\cos(k_{1,0}\cdot r - \omega t + \delta_1), \quad (2)$$

$$\mathbf{E}_{-1,0}(\mathbf{r},t) = \mathbf{E}_{-1,0}\cos(k_{-1,0}\cdot r - \omega t + \delta_1), \quad (3)$$

$$\mathbf{E}_{0,1}(\mathbf{r},t) = \mathbf{E}_{0,1}\cos(k_{0,1}\cdot r - \omega t + \delta_2), \quad (4)$$

$$\mathbf{E}_{0,-1}(\mathbf{r},t) = \mathbf{E}_{0,-1}\cos(k_{0,-1}\cdot r - \omega t + \delta_2), \quad (5)$$

where k and ω are the wave vector and angular frequency of the beam, respectively, E is the constant of electric field strength, and δ is the initial phase of the beam. If the initial phases for five beams are the same, the generated interference pattern has a fcc or fct symmetry.[16–18] In this study, the initial phases for beams (0,1) and $(0,-1)$ are the same but different from those for beams (0,0), (1,0), and $(-1,0)$, i.e., the δ_1 and δ_2 are different in the above equations. This is a consequence of the optical path difference developed between (0,0) and (0,1) [or $(0,\ -1)$] when (0,0) beam goes in a straight line while the (0,1) or $(0,-1)$ travels along a direction with a diffraction angle before further diffracted by the second grating, as shown in Fig. 2(b). The initial phase shift is

$$\delta_2 - \delta_1 = \frac{2\pi}{\lambda} n_{\text{eff}} d\left(\frac{1}{\cos\ \theta} - 1\right),$$

where n_{eff} is the effective refractive index of the phase mask structure, θ is the angle between the wave vectors of beams (0,1) and (0,0), and d is the path length of (0,0) beam passing through the phase mask.

The diffraction efficiency is determined by the cycle, depth and period of the grating structure, the polarization direction of the laser, and the laser wavelength.[24] Experimentally, the cycle and depth of the grating structure can be controlled through the weight percentage of photoinitiator, the laser exposure time, and the sample development time. The period of the grating can be controlled through the interfering angle of the two laser beams. The diffraction efficiency will determine the laser intensity ratio of the zeroth order beam to first order beams, thus determine the contrast in the overall interference pattern.[17]

When one beam goes through the phase mask, nine diffracted beams can be produced. The beams (1,0) and $(-1,0)$ have the same intensity while beams (0,1) and $(0,-1)$ have the same intensity also. The $(\pm 1,\pm 1)$ beams are very weak due to the dual diffractions along the four diagonals and the nonzero incident angle.[24,25] Experimentally, the beam intensities for (0,1) and $(0,-1)$ modes can be different from those for beams (1,0) and $(-1,0)$ due to the diffraction efficiency. As an example, one of the fabricated phase masks generates beam intensities with a ratio of 1: 0.68: 0.38: 0.13 for (0,0), (1,0), (0,1), and (1,1), respectively.

For the five-beam interference pattern with an interfering angle α between beam (0,0) and (0,1), wave vectors are represented by $k_{0,0}=k(0,0,1)$, $k_{1,0}=k(\sin\alpha,\ 0,\ \cos\alpha)$, $k_{-1,0}=k(-\sin\alpha,\ 0,\ \cos\alpha)$, $k_{0,1}=k(0,\ \sin\alpha,\ \cos\alpha)$, and $k_{0,-1}=k(0,\ -\sin\alpha,\ \cos\alpha)$. The interference pattern is determined by the laser intensity modulation I in 3D space,

$$I = \mathbf{E}_{-1,0}\cdot\mathbf{E}_{1,0}\cos[-(4\pi/L)x]$$

$$+ \mathbf{E}_{-1,0} \cdot \mathbf{E}_{0,-1} \cos[-(2\pi/L)x + (2\pi/L)y + (\delta_1 - \delta_2)]$$

$$+ \mathbf{E}_{-1,0} \cdot \mathbf{E}_{0,1} \cos[-(2\pi/L)x - (2\pi/L)y + (\delta_1 - \delta_2)]$$

$$+ \mathbf{E}_{-1,0} \cdot \mathbf{E}_{0,0} \cos[-(2\pi/c)z - (2\pi/L)x]$$

$$+ \mathbf{E}_{1,0}\mathbf{E}_{0,-1} \cos \cdot [(2\pi/L)x + (2\pi/L)y + (\delta_1 - \delta_2)]$$

$$+ \mathbf{E}_{1,0} \cdot \mathbf{E}_{0,1} \cos[(2\pi/L)x - (2\pi/L)y + (\delta_1 - \delta_2)]$$

$$+ \mathbf{E}_{1,0} \cdot \mathbf{E}_{0,0} \cos[-(2\pi/c)z + (2\pi/L)x]$$

$$+ \mathbf{E}_{0,-1} \cdot \mathbf{E}_{0,1} \cos[-(4\pi/L)y]$$

$$+ \mathbf{E}_{0,-1} \cdot \mathbf{E}_{0,0} \cos[-(2\pi/c)z - (2\pi/L)y + (\delta_2 - \delta_1)]$$

$$+ \mathbf{E}_{0,1} \cdot \mathbf{E}_{0,0} \cos[-(2\pi/c)z + (2\pi/L)y + (\delta_2 - \delta_1)], \quad (6)$$

where $L=\lambda/[\sin(a)]$, the periodicity of the interference pattern along x or y direction, and $c=\lambda/[2\sin^2(a/2)]$, the periodicity of the interference pattern along z direction.

There is a way to compensate the intensity difference of these five beams for the five-beam interference. If the polarization of the laser is set to be in [1,0,0] direction, the diffracted beams (1,0) and (−1,0) have polarization directions in xz plane with an angle α relative to x-axis, same as the diffraction angle. The diffracted beams (0,0), (0,1), and (0,−1) have the same polarization as [1,0,0]. Thus $\mathbf{E}_{0,0}\cdot\mathbf{E}_{0,1}$ equals to $E_{0,0}E_{0,1}$; however $\mathbf{E}_{0,0}\cdot\mathbf{E}_{1,0}$ equals to $E_{0,0}E_{1,0}\cos(\alpha)$. Although the beam (1, 0) is stronger than beam (0, 1), the difference between $\mathbf{E}_{0,0}\cdot\mathbf{E}_{0,1}$ and $\mathbf{E}_{0,0}\cdot\mathbf{E}_{1,0}$ becomes small after considering the polarization effect. Thus intensity difference can be compensated by the selection of a polarization for the interference of above five beams when calculating the dot product of two beams.

Figure 3 shows the simulated five-beam interference patterns. The grating period of 1.06 μm was used for the simulation. The beam intensities were set with the values we have measured above, namely, the ratio of beam intensity was set to be 1: 0.68:0.68:0.38:0.38 for (0,0), (1,0), (−1,0), (0,1), and (0,−1). The polarization of the incident laser was set in the [1,0,0] direction. After the diffraction, the polarization for (0,0), (0,1), and (0,−1) beams was set in the [1,0,0] direction. For (1,0) and (−1,0) beams, polarization directions were chosen in xz plane with an angle of 31° relative to x-axis. The maximum phase shift $(\delta_2-\delta_1)$ was estimated to be 0.47π based on the sample thickness of 3 μm. If the phase shift is zero, the low-intensity isointensity surface of the five-beam interference looks like spheroid-type simple fcc or fct structure as shown in Fig. 3(a). With a phase shift of 0.1π, spheroids start to touch each other in one direction [see Fig. 3(b)]. With phase shifts of 0.2π and 0.3π [Figs. 3(c) and 3(d)], the spheroids start to interconnect in two directions and form rods among spheroids. With a phase shift of 0.4π [see Fig. 3(e)], a high isointensity surface forms rods between spheroids and those rods are shifted away from original cross points. Figure 3(f) shows an interference pattern with a phase shift of 0.5π. The pattern has a high intensity around the rods. A layer-by-layer structure is clearly

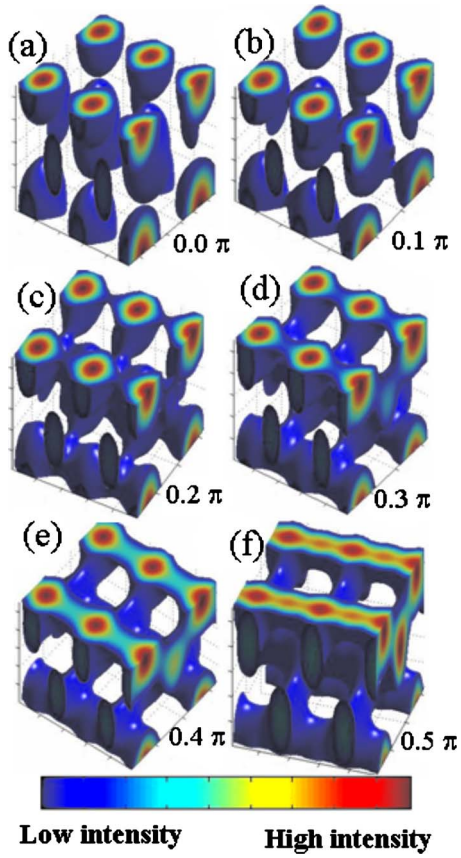

FIG. 3. (Color online) 3D pattern of the five-beam interference with (a) $\delta_2-\delta_1=0\pi$, (b) $\delta_2-\delta_1=0.1\pi$, (c) $\delta_2-\delta_1=0.2\pi$, (d) $\delta_2-\delta_1=0.3\pi$, (e) $\delta_2-\delta_1=0.4\pi$, and (f) $\delta_2-\delta_1=0.5\pi$.

shown. Within each layer, the elliptical rods are arranged with their axes parallel. The orientations of the axes are rotated by 90° between adjacent layers. The elliptical rods of second neighbor are shifted by half lattice constant within the layer in a direction perpendicular to the rod axes. Those are features of a woodpilelike photonic crystal structure. As Chan *et al.*[17] stated, the incorporation of the phase shift for (0,1) and (0,−1) beams is necessary for the formation of diamondlike (woodpilelike) structures. Further increases in the phase shift will transform the structure gradually back to a simple fcc or fct structure.

IV. FABRICATION OF 3D PHOTONIC CRYSTAL USING THE MULTIPLE-LAYER PHASE MASK

The laboratory-fabricated multiple-layer phase mask was used to generate a 3D photonic crystal template in the photoresist mixture with a similar formulation to that described above except that the LC was omitted. The mixture contains DPHPA monomer (84.9%), rose bengal (0.4%), NPG (0.8%), and NVP (13.9%). The mixture was spin coated on the glass slide substrate at a speed of 1000 rpm. The thickness is approximately 15 μm. The phase mask generated beam intensities with a ratio of 1: 0.68: 0.38: 0.13 for (0,0), (1,0), (0,1), and (1,1), respectively. The exposure laser has a wavelength of 532 nm with a polarization in the x-direction [1,0,0]. The photonic crystal template was fabricated in the above photoresist mixture by the single beam and single exposure

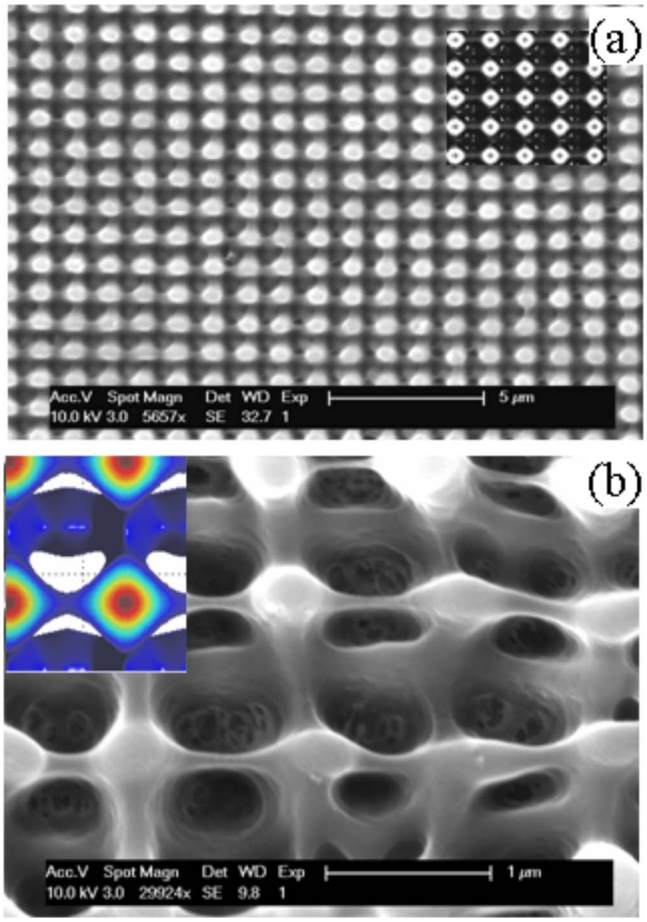

FIG. 4. (Color online) (a) SEM of photonic crystal template fabricated using the multiple-layer phase mask through single beam and single exposure method and (b) the enlarged view of the template. The insets are the simulations of five-beam interference pattern.

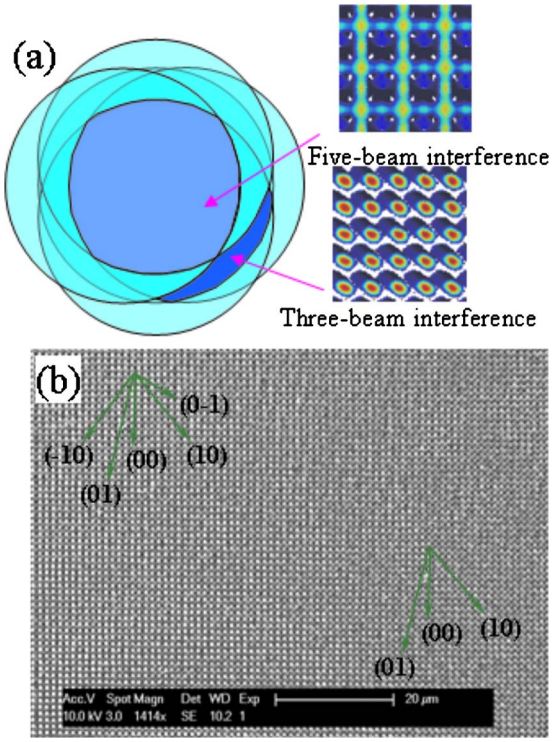

FIG. 5. (Color online) (a) Schematic of beam overlapping showing five-beam interference region, three-beam interference region, and formed interference patterns in these regions. (b) SEM of fabricated photonic crystal template: the top-left region is formed through five beams while the bottom-right region is formed through three beams.

method using the multiple-layer phase mask. The photoresist was placed in a location where five beams overlap. The exposure time was 60 s. The exposed photoresist was developed in PGMEA. Figure 4(a) shows a SEM of the fabricated photonic crystal template. The inset is the simulated structure with parameters similar to those used for Fig. 3 except that a phase shift of 0.35π was used. Figure 4(b) shows an enlarged view of fabricated structure. Again the inset is the simulated structure with a phase shift of 0.35π $(\delta_2-\delta_1=0.35\pi)$. The agreement between the simulation and the fabricated structure is very well. The fabricated structure through the multiple-layer phase mask can only be simulated by an interference pattern with a phase shift, indicating the phase shift among beams generated by the phase mask. From the theory, the period of the structure in Fig. 4 should be the same as the grating period of the phase mask. The measured average period in x and y directions by SEM in Fig. 4(a) is approximately 1.03 μm, compared with the measured grating period of 1.06 μm in Fig. 2(a).

Once the optimal directions, amplitudes, polarizations, and phases are determined, a two-layer phase mask can be designed and fabricated to yield the optimal diffraction condition for the holographic fabrication. The integration of the two-layer phase mask on a single substrate represents a significant improvement toward mass production of 3D photonic structures. Since the two-layer mask can be readily integrated with multiple-layer amplitude mask based IC fabrication, the reported approaches also provide an avenue for chip-scale integration of the 3D photonic devices with other lightwave and electronic circuit elements.

The five beams of (0,0), (1,0), (−1,0), (0,1), (0,−1), and (1,1) can only overlap in a certain region depending on the laser beam size and distance of the sample from the phase mask. Outside five-beam overlapping region, four beams, three beams, or two beams are overlapped in different regions. Figure 5(a) illustrates the five-beam interference region together with three-beam interference and the formed interference patterns in these regions. From the interference patterns, we can see that the symmetry and orientation are totally different from each other in these two regions. Figure 5(b) shows the SEM of the fabricated structure exposed to the interference patterns in these different regions. The top-left region is formed by holographic lithography based on the five-beam interference as can be judged by the tetragonal symmetry of the pattern. The bottom-right region is formed by three-beam interference from beams of (0,0), (1,0), and (0,1). The orientation of the pattern is along the [1,1] direction, in agreement with the theoretical prediction.

V. SUMMARY

In summary, we have demonstrated experimentally the fabrication of a two-layer integrated phase mask and 2D phase mask consisting of two orthogonally oriented gratings. The phase mask was made by double exposure of the pho-

toresist to the laser two-beam interference pattern. For the fabrication of two-layer phase mask, LC was added into the photoresist polymer and the phase separation between LC and the polymer helps preserve the grating produced in the first exposure. The phase relation among the diffracted beams from the two-layer phase mask can be manipulated for the generation of diamondlike photonic crystals. The photonic crystal template has been fabricated by single-exposure, single-beam, optical interference lithography through the two-layer integrated phase mask. The fabricated photonic crystal structure has been compared with the simulated structure. These results indicate a phase shift among the diffracted beams from the two-layer phase mask.

ACKNOWLEDGMENTS

This work is supported by National Science Foundation under Award Nos. CMMI-0609345 (Y.L. and K.L.), DMR-0722754 (Y.L.), and CMMI-0637065 (K.P.C.)

[1]S. John, Phys. Rev. Lett. **58**, 2486 (1987).
[2]E. Yablonovitch, Phys. Rev. Lett. **58**, 2059 (1987).
[3]J. D. Joannopoulos, P. R. Villeneuve, and S. H. Fan, Nature (London) **386**, 143 (1997).
[4]K. M. Ho, C. T. Chan, C. M. Soukoulis, R. Biswas, and M. Sigalas, Solid State Commun. **89**, 413 (1994).
[5]A. Blanco, E. Chomski, S. Grabtchak, M. Ibisate, S. John, S. W. Leonard, C. Lopez, F. Meseguer, H. Miguez, J. P. Mondia, P. Jessica, G. A. Ozin, A. Geoffrey, O. Toader, and H. M. van Driel, Nature (London) **405**, 437 (2000).
[6]M. Deubel, G. V. Freymann, M. Wegener, S. Pereira, K. Busch, and C. M. Soukoulis, Nature Mater. **3**, 444 (2004).
[7]V. Berger, O. Gauthier-Lafaye, and E. Costard, J. Appl. Phys. **82**, 60 (1997).
[8]M. Campbell, D. N. Sharp, M. T. Harrison, R. G. Denning, and A. J. Turberfield, Nature (London) **404**, 53 (2000).
[9]S. Yang, M. Megens, J. Aizenberg, P. Wiltzius, P. M. Chaikin, and W. B. Russel, Chem. Mater. **14**, 2831 (2002).
[10]O. Toader, T. Y. M. Chan, and S. John, Phys. Rev. Lett. **92**, 043905 (2004).
[11]Y. Lin, P. R. Herman, and K. Darmawikarta, Appl. Phys. Lett. **86**, 071117 (2005).
[12]Z. Poole, D. Xu, K. P. Chen, I. Olvera, K. Ohlinger, and Y. Lin, Appl. Phys. Lett. **91**, 251101 (2007).
[13]I. Divliansky, T. S. Mayer, K. S. Holliday, and V. H. Crespi, Appl. Phys. Lett. **82**, 1667 (2003).
[14]Y. V. Miklyaev, D. C. Meisel, A. Blanco, G. V. Freymann, K. Busch, W. Koch, C. Enkrich, M. Deubel, and M. Wegener, Appl. Phys. Lett. **82**, 1284 (2003).
[15]Y. K. Pang, J. C. Lee, C. T. Ho, and W. Y. Tam, Opt. Express **14**, 9013 (2006).
[16]Y. Lin, D. Rivera, Z. Pole, and K. P. Chen, Appl. Opt. **45**, 7971 (2006).
[17]T. Y. M. Chan, O. Toader, and S. John, Phys. Rev. E **73**, 046610 (2006).
[18]Y. Lin, P. R. Herman, and E. L. Abolghasemi, J. Appl. Phys. **97**, 096102 (2005).
[19]C. Zanke, M. Qi, and H. I. Smith, J. Vac. Sci. Technol. B **22**, 3352 (2004).
[20]M. Paturzo, S. Grilla, S. Mailis, G. Coppola, M. Iodice, M. Gioffre, and P. Feeraro, Opt. Commun. **281**, 1950 (2008).
[21]Y. Lin and P. R. Herman, J. Appl. Phys. **98**, 063104 (2005).
[22]R. Jakubiak, L. V. Natarajan, V. Tondiglia, G. S. He, P. N. Prasad, T. J. Bunning, and R. A. Vaia, Appl. Phys. Lett. **85**, 6095 (2004).
[23]V. P. Tondiglia, L. V. Natarajan, R. L. Sutherland, D. Tomlin, and T. J. Bunning, Adv. Mater. (Weinheim, Ger.) **14**, 187 (2002).
[24]S. Peng and G. M. Morris, J. Opt. Soc. Am. A **12**, 1087 (1995).
[25]S. T. Han, Y. Tsao, R. M. Walser, and M. Becker, Appl. Opt. **31**, 2343 (1992).